

Searching for intrinsic charm in the proton at the LHC

V.A. Bednyakov¹, M.A. Demichev¹, G.I. Lykasov¹, T. Stavreva²,
M. Stockton³

¹*Joint Institute for Nuclear Research, Dubna 141980, Moscow region, Russia*

²*Laboratoire de Physique Subatomique et de Cosmologie, UJF,
CNRS/IN2P3, INPG, 53 avenue des Martyrs, 38026 Grenoble, France*

³*Department of Physics, McGill University, Montreal QC, Canada*

Abstract

Despite rather long-term theoretical and experimental studies, the hypothesis of the non-zero intrinsic (or valence-like) heavy quark component of the proton distribution functions has not yet been confirmed or rejected. The LHC with pp -collisions at $\sqrt{s} = 7$ –14 TeV will obviously supply extra unique information concerning the above-mentioned component of the proton. To use the LHC potential, first of all, one should select the parton-level (sub)processes (and final-state signatures) that are most sensitive to the intrinsic heavy quark contributions. To this end inclusive production of $c(b)$ -jets accompanied by photons is considered. On the basis of the performed theoretical study it is demonstrated that the investigation of the intrinsic heavy quark contributions looks very promising at the LHC in processes such as $pp \rightarrow \gamma + c(b) + X$.

1. Introduction

The Large Hadron Collider (LHC) opens up new and unique kinematical regions with high accuracy for the investigation of the structure of the proton, in particular for the study of the parton distribution functions (PDFs). It is well known that the precise knowledge of the PDFs is essential for the verification of the Standard Model and the search for New Physics.

By definition, the PDF $f_a(x, \mu)$ is a function of the proton momentum fraction x carried by parton a (quark q or gluon g) at the momentum transfer scale μ . For small values of μ , corresponding to long distance scales less than $1/\mu_0$, the PDF currently cannot be calculated from first principles. [1]. At $\mu > \mu_0$ the $f_a(x, \mu)$ can be obtained by means of solving the perturbative QCD evolution equations (DGLAP) [2]. At $\mu < \mu_0$ some progress in the calculation of the PDFs has been achieved within lattice methods [1]. The unknown (input for the evolution) functions $f_a(x, \mu_0)$ usually can be found empirically from some ‘‘QCD global analysis’’ [3, 4] of a large variety of data typically at $\mu > \mu_0$.

In general, almost all pp processes at LHC energies, including Higgs boson production, are sensitive to the charm $f_c(x, \mu)$ or bottom $f_b(x, \mu)$ PDFs. Nevertheless,

within the global analyses the charm content of the proton at $\mu \sim \mu_c$ and the bottom at $\mu \sim \mu_b$ are both assumed to be negligible. Here μ_c and μ_b are typical energy scales relevant to the c - and b -quark QCD excitation in the proton. These heavy quark components arise in the proton only perturbatively with increases in the Q^2 -scale through gluon splitting in the DGLAP Q^2 evolution [2]. Direct measurement of open charm and open bottom production in deep inelastic processes (DIS) confirms the perturbative origin of heavy quark flavours [5]. However, modern descriptions of these experimental data are not sensitive enough to the above-mentioned perturbative sea heavy quark distributions at relatively large x values ($x > 0.1$).

Analyzing hadroproduction of the so-called leading hadrons Brodsky et al. [6, 7] (about thirty years ago) have assumed the co-existence of *extrinsic* and *intrinsic* contributions to the quark-gluon structure of the proton. The *extrinsic* (or ordinary) quarks and gluons are generated on a short time scale associated with large-transverse-momentum processes. Their distribution functions satisfy the standard QCD evolution equations. The *intrinsic* quarks and gluons exist over a time scale which is independent of any probe momentum transfer. They can be associated with a bound-state (zero-momentum transfer regime) hadron dynamics and one believes they have a nonperturbative origin.

It was shown in [7] that the existence of *intrinsic* heavy quark pairs $c\bar{c}$, and $b\bar{b}$ within the proton state can be due to the virtue of gluon-exchange and vacuum-polarization graphs. On this basis, within the MIT bag model [8], the probability to find a five-quark component $|uudc\bar{c}\rangle$ bound within the nucleon bag is nonzero and can be about 1–2%.

Initially in [6, 7] S. Brodsky and coauthors proposed the existence of the 5-quark state $|uudc\bar{c}\rangle$ in the proton. Later some other models were developed. One of them considered a quasi-two-body state $\bar{D}^0(u\bar{c})\bar{\Lambda}_c^+(udc)$ in the proton [9]. In order to not contradict the DIS HERA data the probability to find the intrinsic charm (IC) in the proton (the weight of the relevant Fock state in the proton) was found to be less than 3.5% [9]–[12]. The probability of finding an intrinsic bottom (IB) state in the proton is suppressed by a factor of $m_c^2/m_b^2 \simeq 0.1$ [13], where $m_c \simeq 1.3$ GeV and $m_b = 4.2$ GeV are the current masses of the charm and bottom quarks. Therefore, the experimental search for a possible IC signal in pp collisions at the LHC is more promising than the search for the IB contribution.

If the distributions of the intrinsic charm or bottom in the proton are hard enough and similar in shape to the valence quark distributions (i.e. have valence-like form), then one expects the production of charmed (bottom) mesons or charmed (bottom) baryons in the fragmentation region to be similar to the production of pions or nucleons (from the light quarks). However, the yield of this production depends on the probability to find intrinsic charm or bottom in the proton, but this amount looks too small. The PDFs that include the IC contribution in the proton have already been used in perturbative QCD calculations in [9]–[12].

The probability distribution for the 5-quark state ($|uudc\bar{c}\rangle$) in the light-cone description of the proton was first calculated in [6]. The general form for this

distribution calculated within the light-cone dynamics in the so-called BHPS model [6, 7] can be written as [11]

$$P(x_1, \dots, x_5) = N_5 \delta \left(1 - \sum_{j=1}^5 x_j \right) \left(m_p^2 - \sum_{j=1}^5 \frac{m_j^2}{x_j} \right)^{-2}, \quad (1)$$

where x_j is the momentum fraction of the parton, m_j is its mass and m_p is the proton mass. Neglecting the light quark (u, d, s) masses and the proton mass in comparison to the c -quark mass and integrating (1) over $dx_1 \dots dx_4$ one can get the probability to find intrinsic charm with momentum fraction x_5 in the proton [11]:

$$P(x_5) = \frac{1}{2} \tilde{N}_5 x_5^2 \left\{ \frac{1}{3} (1 - x_5)(1 + 10x_5 + x_5^2) - 2x_5(1 + x_5) \ln(x_5) \right\}, \quad (2)$$

where $\tilde{N}_5 = N_5/m_{4,5}^4$, $m_{4,5} = m_c = m_{\bar{c}}$, the normalization constant N_5 determines some probability w_{IC} to find the Fock state $|uudc\bar{c}\rangle$ in the proton. Figure 1 illustrates the IC contribution in comparison to the conventional sea charm quark distribution in the proton.

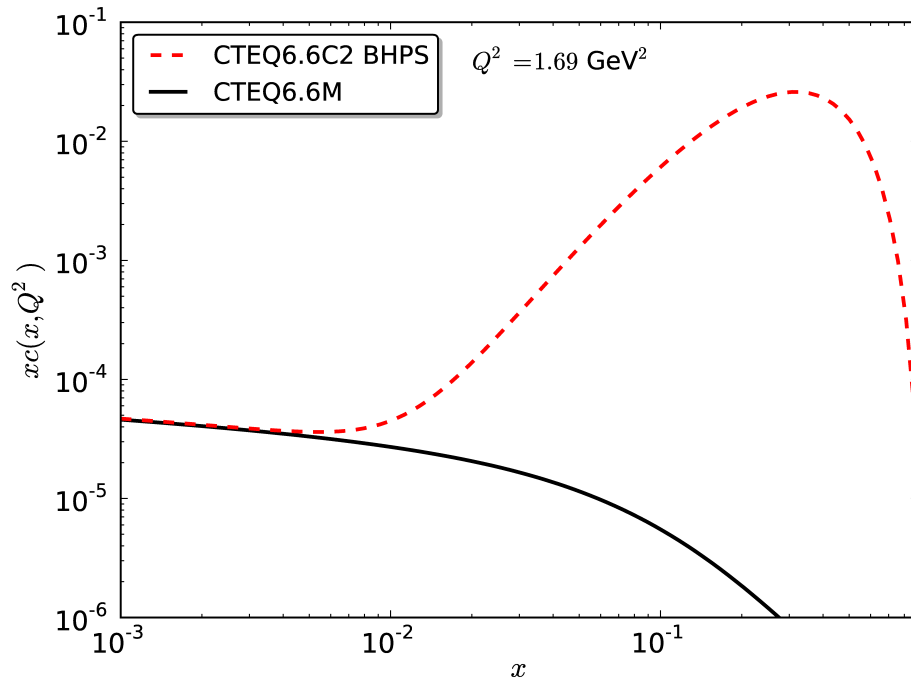


Figure 1: Distributions of the charm quark in the proton. The solid line is the radiatively generated charm density distribution $x_{c_{\text{rg}}}(x)$ only, whereas the dashed curve is a full charm quark distribution function, i.e. the sum of the intrinsic charm density $x_{c_{\text{in}}}(x)$ (see (2)) and $x_{c_{\text{rg}}}(x)$.

The solid line in Fig. 1 shows the radiatively generated charm density distribution $xc_{\text{rg}}(x)$ (ordinary sea charm) in the proton from CTEQ6.6M [12] as a function of x at $Q^2 = m_c^2 = (1.3)^2 \text{ (GeV}/c)^2$. The dashed curve in Fig. 1 is the sum of the intrinsic charm density $xc_{\text{in}}(x)$ with the IC probability $w_{\text{IC}} = 3.5\%$ and $xc_{\text{rg}}(x)$ at the same $Q^2 = m_c^2$, CTEQ6.6C2 BHPS [12]. One can see from Fig. 1 that the IC distribution (with $w_{\text{IC}} = 3.5\%$) given by (2) has a rather visible enhancement at $x \sim 0.2\text{--}0.3$ and this distribution is much larger (by a few orders of magnitude) than the sea (ordinary) charm density distribution in the proton.

As a rule, the gluons and sea quarks play the key role in hard processes of open charm hadroproduction. Simultaneously, due to the nonperturbative *intrinsic* heavy quark components one can expect some excess of these heavy quark PDFs over the ordinary sea quark PDFs at $x > 0.1$. Therefore the existence of the intrinsic charm component can lead to some enhancement in the inclusive spectra of open charm hadrons, in particular D -mesons, produced at the LHC in pp -collisions at large pseudorapidities η and large transverse momenta p_T [15]. Furthermore, as we know from [6]–[12] photons produced in association with heavy quarks $Q(\equiv c, b)$ in the final state of pp -collisions provide valuable information about the parton distributions in the proton [9]–[24].

In this paper, having in mind these considerations we will first discuss where the above-mentioned heavy flavour Fock states in the proton could be searched for at the LHC. Following this we analyze in detail, and give predictions for the LHC semi-inclusive pp -production of prompt photons accompanied by c -jets including the *intrinsic* charm component in the PDF.

For completeness, in these predictions the sea-like charm PDF [10] is also considered. As described in [10] this is a purely phenomenological scenario, where the intrinsic sea-like charm at the initial scale $Q_0 = m_c$ is believed to be proportional to the light sea PDFs, i.e. $c(x) = \bar{c}(x) \sim \bar{u}(x) + \bar{d}(x)$. This distribution tends to be enhanced at most x -values when compared to the ordinary charm distribution (CTEQ6.6M).

2. The intrinsic charm and beauty

According to the model of hard scattering [25]–[33] the relativistic invariant inclusive spectrum of the hard process $p + p \rightarrow h + X$ can be related to the elastic parton-parton subprocess $i + j \rightarrow i' + j'$, where i, j are the partons (quarks and gluons), by the formula [29]–[31]:

$$E \frac{d\sigma}{d^3p} = \sum_{i,j} \int d^2k_{iT} \int d^2k_{jT} \int_{x_i^{\text{min}}}^1 dx_i \int_{x_j^{\text{min}}}^1 dx_j f_i(x_i, k_{iT}) f_j(x_j, k_{jT}) \frac{d\sigma_{ij}(\hat{s}, \hat{t})}{d\hat{t}} \frac{D_{i,j}^h(z_h)}{\pi z_h}. \quad (3)$$

Here: $k_{i,j}$ and $k'_{i,j}$ are the four-momenta of the partons i or j before and after the elastic parton-parton scattering, respectively; k_{iT}, k_{jT} are the transverse momenta of the partons i and j ; $f_{i,j}$ are the PDFs of partons i, j inside the proton; $D_{i,j}^h$ is

the fragmentation function (FF) of the parton i or j to a hadron h ; and z_h is the fraction of the final state hadron momentum from the parton momentum.

When the transverse momenta of the partons are neglected in comparison to the longitudinal momenta, the variables \hat{s} , \hat{t} , \hat{u} and z_h can be presented in the following form [29]: $\hat{s} = x_i x_j s$, $\hat{t} = x_i \frac{t}{z_h}$, $\hat{u} = x_j \frac{u}{z_h}$, $z_h = \frac{x_1}{x_i} + \frac{x_2}{x_j}$, where,

$$x_1 = -\frac{u}{s} = \frac{x_T}{2} \cot(\theta/2), \quad x_2 = -\frac{t}{s} = \frac{x_T}{2} \tan(\theta/2), \quad x_T = 2\sqrt{tu}/s = 2p_T/\sqrt{s}. \quad (4)$$

Here as usual, $s = (p_1 + p_2)^2$, $t = (p_1 - p'_1)^2$, $u = (p_2 - p'_1)^2$, and p_1 , p_2 , p'_1 are the 4-momenta of the colliding protons and the produced hadron h , respectively; θ is the scattering angle of hadron h in the pp c.m.s. The lower limits of the integration in (3) are

$$x_i^{\min} = \frac{x_T \cot(\frac{\theta}{2})}{2 - x_T \tan(\frac{\theta}{2})}, \quad x_j^{\min} = \frac{x_i x_T \tan(\frac{\theta}{2})}{2x_i - x_T \cot(\frac{\theta}{2})}. \quad (5)$$

One can see that the Feynman variable x_F of the produced hadron, for example the D -meson, can be expressed via the variables p_T and η , or θ being the hadron scattering angle in the pp c.m.s:

$$x_F \equiv \frac{2p_z}{\sqrt{s}} = \frac{2p_T}{\sqrt{s}} \frac{1}{\tan \theta} = \frac{2p_T}{\sqrt{s}} \sinh(\eta). \quad (6)$$

With (6) the low limit x_i^{\min} in (3) has the following equivalent form:

$$x_i^{\min} = \frac{x_R + x_F}{2 - (x_R - x_F)}, \quad (7)$$

where $x_R = 2p/\sqrt{s}$. One can see from (7) that, at least, one of the low limits x_i^{\min} of the integral (3) must be $\geq x_F$. Thus if $x_F \geq 0.1$, then $x_i^{\min} > 0.1$, where the ordinary (*extrinsic*) charm distribution is completely negligible in comparison with the *intrinsic* charm distribution. Therefore, at $x_F \geq 0.1$, or equivalently at the charm momentum fraction $x_c > 0.1$ the *intrinsic* charm distribution intensifies the charm PDF contribution into charm hadroproduction substantially (see Fig. 1). As a result, the spectrum of the open charm hadroproduction can be increased in a certain region of p_T and η (which corresponds to $x_F \geq 0.1$ in accordance to (7)). We stress that this excess (or even the very possibility to observe relevant events in this region) is due to the non-zero contribution of the IC component at $x_c > x_F > 0.1$ (where the non-IC component is much smaller).

This possibility was demonstrated for the D -meson production at the LHC in [15]. It was shown that the p_T spectrum of D -mesons is enhanced at pseudorapidities of $3 < \eta < 5.5$ and $10 \text{ GeV}/c < p_T < 25 \text{ GeV}/c$ due to the IC contribution, which was included using the CTEQ66c PDF [12]. For example, due to the IC PDF, with

probability about 3.5 %, the p_T -spectrum increases by a factor of 2 at $\eta = 4.5$. A similar effect was predicted in [34].

One expects a similar enhancement in the experimental spectra of the open bottom production due to the (hidden) IB in the proton, which could have a distribution very similar to the one given in (2). However, the probability w_{IB} to find the Fock state with the IB contribution $|uudb\bar{b}\rangle$ in the proton is about 10 times smaller than the IC probability w_{IC} due to the relation $w_{\text{IB}}/w_{\text{IC}} \sim m_c^2/m_b^2$ [7, 13].

The IC “signal” can be studied not only in the inclusive open (forward) charm hadroproduction at the LHC, but also in some other processes, such as production of real prompt photons γ or virtual ones γ^* , or Z^0 -bosons (decaying into dileptons) accompanied by c -jets in the kinematics available to the ATLAS and CMS experiments. The contributions of the heavy quark states in the proton could be investigated also in the $c(b)$ -jet production accompanied by the vector bosons W^\pm, Z^0 . Similar kinematics given by (6) and (7) can also be applied to these hard processes.

In the next section we analyze in detail the hard process of real photon production in pp collision at the LHC accompanied by a c -jet including the IC contribution in the proton.

3. Prompt photon and c -jet production

Recently the investigation of prompt photon and $c(b)$ -jet production in $p\bar{p}$ collisions at $\sqrt{s} = 1.96$ TeV was carried out at the TEVATRON [18]-[21]. In particular, it was observed that the ratio of the experimental spectrum of the prompt photons, (accompanied by the c -jets) to the relevant theoretical expectation (based on the conventional PDF which ignored the *intrinsic* charm) increases with p_T^γ up to a factor of about 3 when p_T^γ reaches 110 GeV/ c . Furthermore, taking into account the CTEQ66c PDF, which includes the IC contribution obtained within the BHPS model [6, 7] one can reduce the difference down to a factor of around 1.5-2 [36]. For the $\gamma + b$ -jets $p\bar{p}$ -production no enhancement in the p_T^γ -spectrum was observed at the beginning of the experiment [18, 21]. However in 2012 the DØ collaboration has confirmed observation of such an enhancement [20].

This intriguing observation stimulates our interest to look for a similar “IC signal” in $pp \rightarrow \gamma + c(b) + X$ processes at the LHC.

The LO QCD Feynman diagrams for the process $c(b) + g \rightarrow \gamma + c(b)$ are presented in Fig. 2. These hard sub-processes give the main contribution to the reaction $pp \rightarrow \gamma + c(b)\text{-jet} + X$.

The inclusive spectrum of prompt photons produced in pp collisions as a function of their transverse momentum p_T^γ is calculated in a similar way to the D -meson spectrum (3). The calculations include the IC contribution through the use of the CTEQ66c PDFs [12]. The hard parton-parton cross section (entering (3)) for the

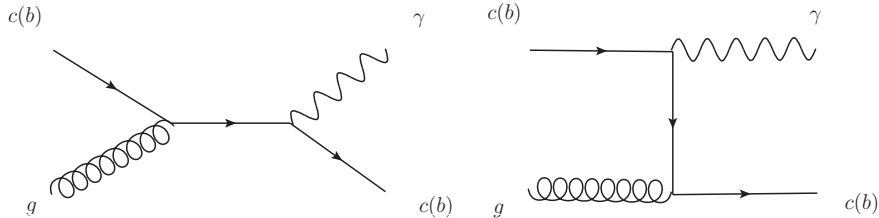


Figure 2: The Feynman diagrams for the hard process $c(b)g \rightarrow \gamma c(b)$, the one-quark exchange in the s-channel (left) and the same in the t-channel (right).

process $gq \rightarrow \gamma q$ is used in the LO QCD form [31]:

$$\frac{d\sigma_{gq \rightarrow \gamma q}(\hat{s}, \hat{t})}{d\hat{t}} = \frac{8\pi}{\hat{s}^2} \alpha_{em} \alpha_s(Q^2) \times \left\{ -\frac{e_q^2}{3} \left(\frac{\hat{u}}{\hat{s}} + \frac{\hat{s}}{\hat{u}} \right) \right\}, \quad (8)$$

where α_{em} is the electromagnetic coupling constant, $\alpha_s(Q^2)$ is the QCD running coupling constant obtained within LO QCD, e_q is the quark charge and $Q^2 = 2\hat{s}\hat{t}\hat{u}/(\hat{s}^2 + \hat{t}^2 + \hat{u}^2)$. Within LO QCD, in addition to the main subprocesses illustrated in Fig. 2 one considers the subprocesses $gg \rightarrow c\bar{c}$, $qc \rightarrow qc$, $gc \rightarrow gc$ accompanied by the bremsstrahlung $c(\bar{c}) \rightarrow c\gamma$, the contribution of which is sizable at low p_T^γ and can be neglected at $p_T^\gamma > 60$ GeV/c, according to [37]. The diagrams within the NLO QCD are more complicated than Fig. 2.

Let us illustrate qualitatively the kinematical regions where the IC component can contribute significantly to the spectrum of prompt photons produced together with a c -jet in pp collisions at the LHC. For simplicity we consider only the contribution to the reaction $pp \rightarrow \gamma + c(\text{jet}) + X$ of the diagrams given in Fig. 2. According to (6) and (7), at certain values of the transverse momentum of the photon, p_T^γ , and its pseudo-rapidity, η_γ , (or rapidity y_γ) the momentum fraction of γ can be $x_{F\gamma} > 0.1$, therefore the fraction of the initial c -quark must also be above 0.1, where the IC contribution in the proton is enhanced (see Fig. 1). Therefore, one can expect some non-zero IC signal in the p_T^γ spectrum of the reaction $pp \rightarrow \gamma + c + X$ in this certain region of p_T^γ and y_γ . In principle, a similar qualitative IC effect can be visible in the production of γ^*/Z^0 decaying into dileptons accompanied by c -jets in pp collisions.

In Fig. 3 the distribution $d\sigma/dp_T^\gamma$ of prompt photons produced in the reaction $pp \rightarrow \gamma + c + X$ at $\sqrt{s} = 8$ TeV is presented for the photon rapidity interval $1.52 < |y_\gamma| < 2.37$ and for c -jet rapidity $|y_c| < 2.4$. The calculation was carried out within PYTHIA8 [38] and only the diagrams in Fig. 2 are included.

The upper line in the top of Fig. 3 is calculated with the use of the CTEQ66c PDF and includes IC, while the lower line uses the CTEQ66 PDF where the charm PDF is radiatively generated only. The probability of the IC contribution is about 3.5% [12]. The ratio of the spectra with IC and without IC as a function of p_T^γ is presented in the bottom of Fig. 3.

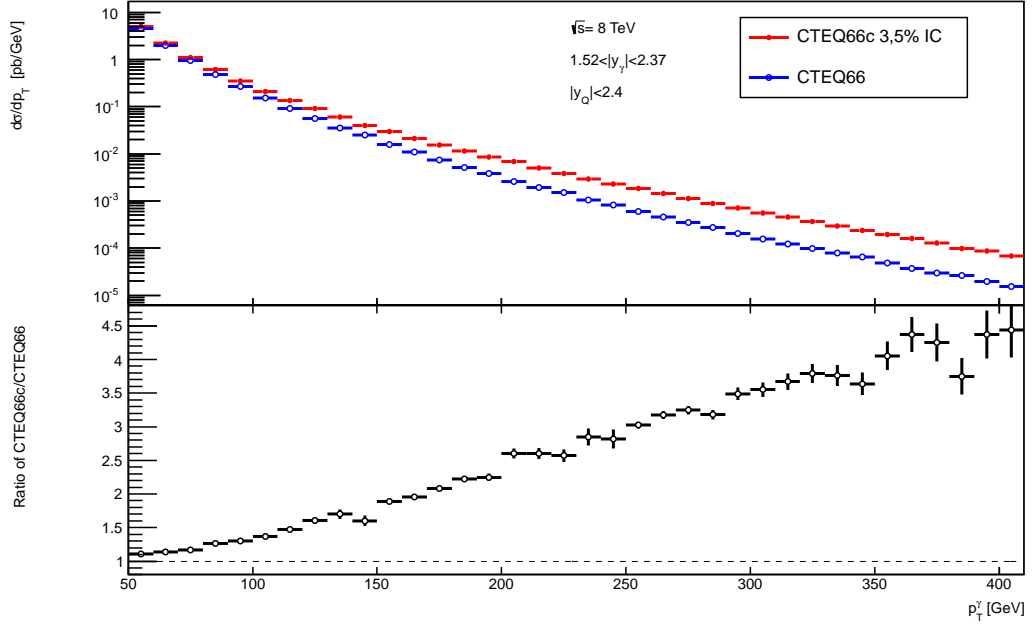


Figure 3: The PYTHIA8 calculation of the distribution $d\sigma/dp_T^\gamma$ for prompt photons from the reaction $pp \rightarrow \gamma cX$ with transverse momentum p_T^γ , in the interval $1.52 < |y_\gamma| < 2.37$, $|y_c| < 2.4$ and at $\sqrt{s} = 8$ TeV including the hard sub-process $g + c \rightarrow \gamma + c$ (Fig. 2). The red solid points (upper points) correspond to the inclusion of the IC contribution in the CTEQ66c PDF with IC probability of about 3.5% [12]; the blue open points (lower line) represent the cross-section calculated using the CTEQ66 PDF without the IC contribution.

One can see from Fig. 3 that the inclusion of the IC contribution increases the spectrum by a factor of 4-4.5 at $p_T^\gamma \simeq 400$ GeV/c, however the cross section is too small here (about 1 fb). At $p_T^\gamma \simeq 150$ -200 GeV/c the cross section is about 8–30 fb if the IC is included and the IC signal reaches 250% - 300%. It corresponds to 800–3000 events in the 5 GeV/c bin for a luminosity $L = 20$ fb $^{-1}$.

Naturally the p_T^γ distribution in Fig. 3 has the same form as the distribution over the transverse momentum of the c -quark, p_T^c , when only the hard subprocess $g + c \rightarrow \gamma + c$ in Fig. 2 is included.

In Fig. 4 the same distributions as in Fig. 3 are presented including the radiation corrections for the initial (ISR) and final (FSR) states along with the multi-parton interactions (MPI) within PYTHIA8.

According to this figure, the IC signal can be about 180%-250% at $p_T^\gamma \simeq 150$ -200 GeV/c and the cross section is about 10–40 fb, which corresponds to about 1000–4000 events in the 5 GeV/c bin at $L=20$ fb $^{-1}$.

Comparing Fig. 3 and Fig. 4 one can conclude that the inclusion of the ISR,

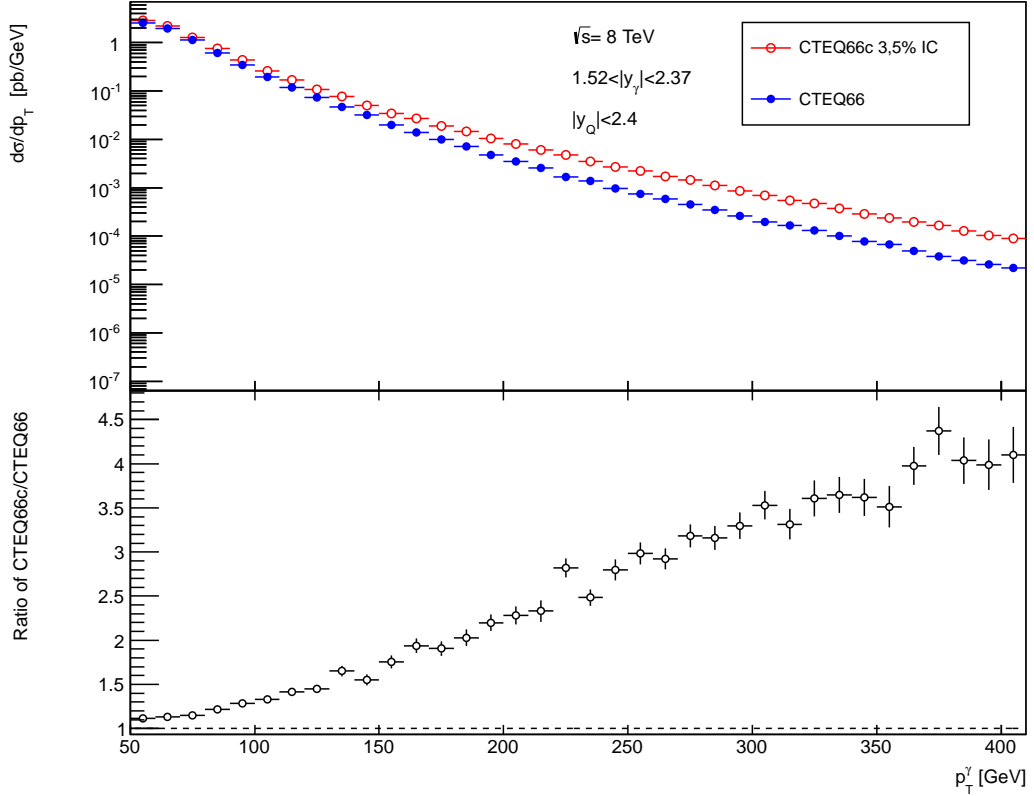


Figure 4: The distribution $d\sigma/dp_T^\gamma$ of prompt photons produced in the reaction $pp \rightarrow \gamma cX$ over the transverse momentum p_T^γ integrated over dy in the interval $1.52 < |y_\gamma| < 2.37$, $|y_c| < 2.4$ at $\sqrt{s} = 8$ TeV. The red open points correspond to the inclusion of the IC contribution in the CTEQ66c PDF with IC probability of about 3.5% [12]; the blue solid points represent the cross-section calculated using the CTEQ66 PDF without the IC contribution. The calculation was done within PYTHIA8 using the LO QCD and including the ISR, FSR and MPI.

FSR and the MPI decreases the cross section at $p_T^\gamma \simeq 50-100$ GeV/c and increases a little bit at $p_T^\gamma \simeq > 100$ GeV/c.

In Fig. 5 the differential cross-section $d\sigma/dp_T^\gamma$ calculated at NLO in the massless quark approximation as described in [36] is presented as a function of the transverse momentum of the prompt photon. The following cuts are applied: $p_T^\gamma > 45$ GeV, $p_T^c > 20$ GeV with the c -jet pseudorapidity in the interval $|y_c| \leq 2.4$ and the photon pseudorapidity in the central region $|y_\gamma| < 1.37$.

The solid blue line represents the differential cross-section calculated with the radiatively generated charm PDF (CTEQ66), the dash-dotted green line uses as input the sea-like PDF (CTEQ66c4) and the dashed red line the BHPS PDF (CTEQ66c2). In the lower half of Fig. 5 the above distributions normalized to the distribution ac-

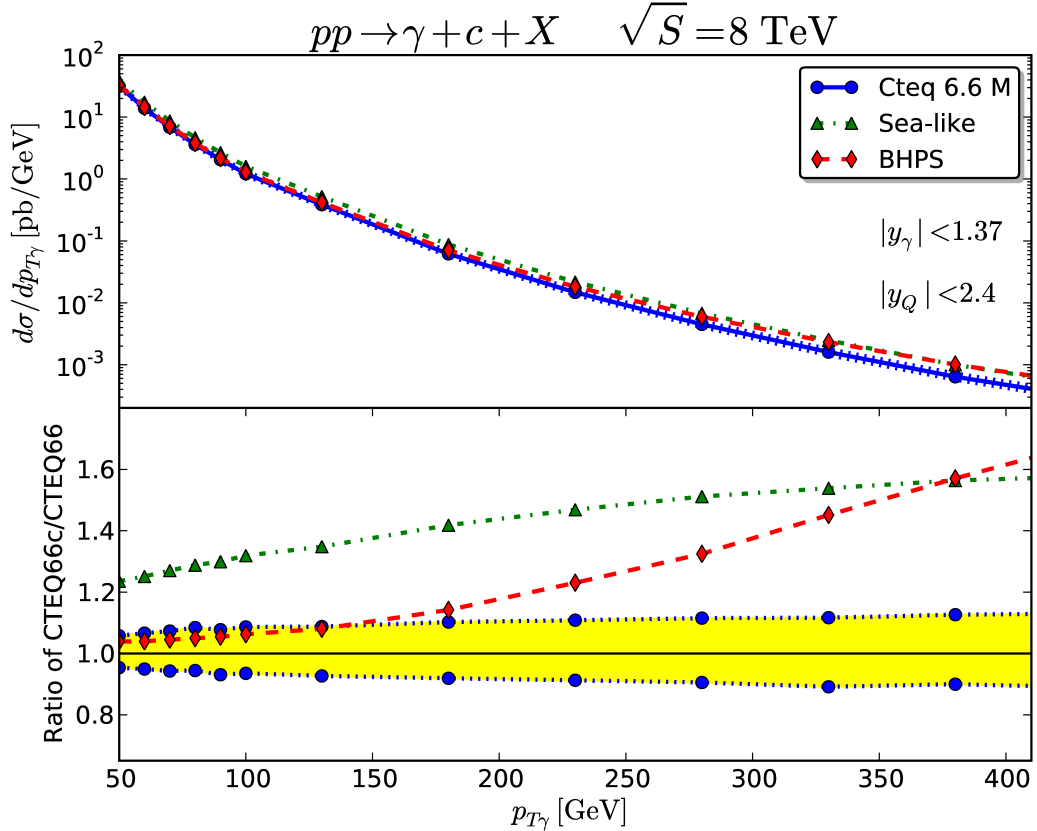


Figure 5: The $d\sigma/dp_T^\gamma$ distribution versus the transverse momentum of the photon for the process $pp \rightarrow \gamma + c + X$ at $\sqrt{s} = 8$ TeV using CTEQ6.6M (solid blue line), BHPS CTEQ6c2 (dashed red line) and sea-like CTEQ6c4 (dash-dotted green line), for central photon rapidity $|y_\gamma| < 1.37$ (top). The ratio of these spectra with respect to the CTEQ6.6M (solid blue line) distributions (bottom). The calculation was done within the NLO QCD approximation.

quired using the CTEQ66 PDF and $\mu_r = \mu_f = \mu_F = p_T^\gamma$, are presented. The shaded yellow region, represents the scale dependence. Clearly the difference between the spectrum using the BHPS IC PDF and the one using the radiatively generated PDF increases as p_T^γ increases, however in this central rapidity region at $p_T^\gamma \sim 400$ GeV the BHPS IC and sea-like IC spectra are roughly the same.

In Fig. 6 the same distributions as in Fig. 5 are shown, however for forward photon rapidity $1.52 < |y_\gamma| < 2.37$. In this case larger - x values are probed and therefore we start to observe the difference between the solid and dashed (dash-dotted) lines at smaller p_T^γ values than in Fig. 5. The difference when using the BHPS IC PDFs is about 200% at $p_T^\gamma \sim 200$ GeV and increases almost up to 300% for $p_T^\gamma \sim 400$ GeV. In this rapidity region the difference between the BHPS and sea-like spectra is clearly visible even as early as $p_T^\gamma \sim 200$ GeV. However, while the IC is more accentuated, the cross-section and hence the number of events is less

than those for the photon central rapidity in Fig. 5.

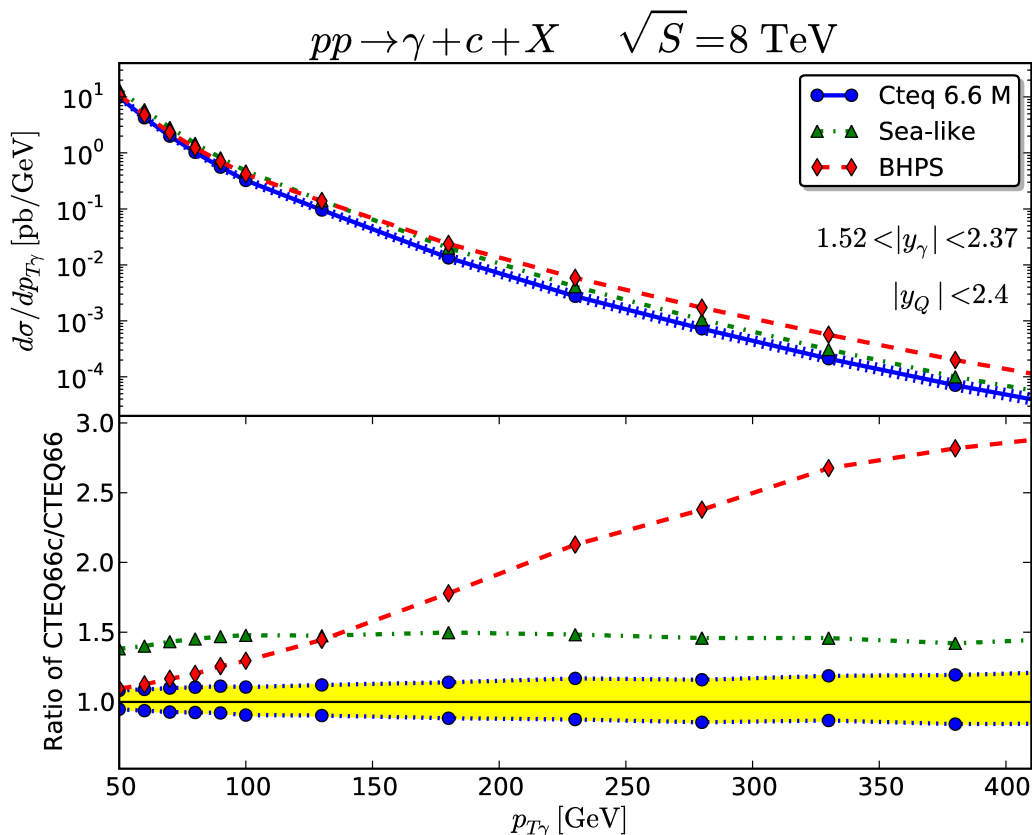


Figure 6: The $d\sigma/dp_T^\gamma$ distribution versus the transverse momentum of the photon for the process $pp \rightarrow \gamma + c + X$ at $\sqrt{s} = 8$ TeV using CTEQ6.6M (solid blue line), BHPS CTEQ6c2 (dashed red line) and sea-like CTEQ6c4 (dash-dotted green line), for forward photon rapidity $1.52 < |y_\gamma| < 2.37$ (top). The ratio of these spectra with respect to the CTEQ6.6M (solid blue line) distributions (bottom). The calculation was done within the NLO QCD approximation.

Comparing Figs. 3,4 to Figs. 5,6 one can see that both the LO QCD and NLO QCD cross-section result in approximately the same IC contribution, which increases when the photon transverse momentum grows. Nevertheless the values of the spectra calculated within the NLO QCD are larger by a factor of about 1.3 than the ones obtained within the LO QCD at $p_T^\gamma > 100$ GeV/c including the ISR, FSR and the MPI. Note that all the calculations presented in Figs. (3-6) were done for isolated photons.

Therefore Figs 3–6 show that the IC signal could be visible at the LHC with both the ATLAS and CMS detectors in the process $pp \rightarrow \gamma + c + X$ when $p_T^\gamma \simeq 150$ GeV/c. In this region the IC signal dominates over all non-intrinsic charm background with significance at a level of a factor of 2 (more precisely 170%).

4. Conclusions

In this paper we have shown that the possible existence of the intrinsic heavy quark components in the proton can be seen not only in the forward open heavy flavor production in pp -collisions (as it was believed before) but it can be visible also in the semi-inclusive pp -production of prompt photons and c -jets at rapidities $1.5 < |y_\gamma| < 2.4$, $|y_c| < 2.4$ and large transverse momenta of photons and jets. In the inclusive photon spectrum measured together with a c -jet a rather visible enhancement can appear due to the intrinsic charm (IC) quark contribution. In particular, it was shown that the IC contribution can produce much more events (factor 2 or 3) at $p_T^\gamma > 150$ GeV/ c and forward y_γ in comparison with the the relevant number expected in the absence of the IC. Furthermore the same enhancement is also coherently expected in the transverse momentum, p_T^c , distribution of the c -jet measured together with the above-mentioned prompt photon in the $pp \rightarrow \gamma + c\text{-jet} + X$ process.

Searching for the signal of *intrinsic* charm in such processes is more pronounced than the search for the *intrinsic* bottom because the IB probability is, at least, 10 times smaller than the IC probability in the proton.

Our predictions can be verified at the LHC by the ATLAS and CMS Collaborations. To this end further consideration of non-charm (light quarks) backgrounds for the discussed processes is mandatory.

Acknowledgments

We thank S.J. Brodsky and A.A. Glasov for extremely helpful discussions and recommendations by the study of this topic. The authors are grateful to H. Jung, A.V. Lipatov, V.A.M. Radescu, A. Sarkar and N.P. Zotov for very useful discussions and comments. This research was also supported by the RFBR grants No. 11-02-01538-a and No. 13-02001060.

References

- [1] J.W. Negele *et al.*, Nucl.Phys. B [Proc.Suppl.] **128**, (2004) 170; W.Schroers, Nucl. Phys. A **755** (2005) 333.
- [2] V.N. Gribov and L.N. Lipatov, Sov.J.Nucl.Phys. **15** (1972) 438; G. Altarelli and G. Parisi, Nucl.Phys. B **126** (1997) 298; Yu.L. Dokshitzer, Sov.Phys. JETP **46** (1977) 641.
- [3] J. Pumplin, D.R. Stump, J. Huston, H.L. Lai, P. Nadolsky and W.K. Tung, J. High Energy Physics **07** (2002) 012; D.R. Stump, J. Huston, J. Pumplin, W.K. Tung, H.L. Lai, S. Kuhlmann and J.F. Owens, J. High Energy Physics **10** (2003) 046.
- [4] R.S. Thorne, A.D. Martin, W.J. Stirling, and R.G. Roberts, arXiv:0407311 [hep-ph].
- [5] A. Aktas, *et al.*, (H1 Collaboration), Eur.Phys. J.C40, (2005) 349; arXiv:0507081 [hep-ex].
- [6] S. Brodsky, P. Hoyer, C. Peterson, N. Sakai, Phys.Lett. B **93** (1980) 451.
- [7] S. Brodsky, C. Peterson, N. Sakai, Phys.Rev. D, **23** (1981) 2745.
- [8] J.F. Donoghue, E. Golowich, Phys.Rev.D **15** (1977) 3421.

- [9] J. Pumplin, Phys.Rev. D **73** (2006) 114015.
- [10] J. Pumplin, H.L. Lai, W.K. Tung, Phys.Rev. D **75** (2007) 054029.
- [11] Jen-Chien Peng, Wen-Chen Chang, Sixth Intern. Conf., on Quarks and Nuclear Physics, April 16-20, 2012, Ecole Polytechnique Palaiseau, Paris, arXiv:1207.2193 [hep-ph].
- [12] P.M. Nadolsky, *et al.*, Phys. Rev. D **78** (2008) 013004.
- [13] M.V. Polyakov, A. Schafer, O.V. Teryaev, Phys.Rev. D **60** (1999) 051502.
- [14] V. Goncalves, F. Navarra, Nucl.Phys. A **842** (2010) 59.
- [15] G.I. Lykasov, V.A. Bednyakov, A.F. Pikelner and N.I. Zimin, Eur.Phys.Lett. **99** (2012) 21002; arXiv:1205.1131v2 [hep-ph].
- [16] Jen-Chieh Peng, Wen-Chen Chang, arXiv:1207.2193 [hep-ph].
- [17] V.A. Litvine, A.K. Likhoded, Phys. Atom. Nucl. **62** (1999) 679.
- [18] V.M. Abazov, *et al.*, Phys.Rev.Lett. **102** (2009) 192002; arXiv:0901.0739 [hep-ex].
- [19] V.M. Abazov, *et al.*, Phys.Lett. B **719** (2013) 354; arXiv:1210.5033 [hep-ex].
- [20] V.M. Abazov, *et al.*, Phys.Lett. B **714** (2012) 32; arXiv:1203.5865 [hep-ex].
- [21] T. Aaltonen, *et al.*, Phys.Rev. D **81** (2010) 052006; arXiv:0912.3453 [hep-ex].
- [22] R. Vogt, Prog. Part. Nucl. Phys. **45** (2000) S105.
- [23] F.S. Navarra, M. Nielsen, C.A.A. Nunes, Teixeira M., Phys.Rev. D **54** (1996) 842.
- [24] W. Melnichouk, A.W. Thomas, Phys.Lett. B **414** (1997) 134.
- [25] A.V. Efremov, Sov.J.Nucl.Phys., **19**, 176 (1974).
- [26] P. Nason, S. Dawson and R.K. Ellis, Nucl.Phys., B **303**, 607 (1988).
- [27] P. Nason, S. Dawson and R.K. Ellis, Nucl.Phys., B **327**, 49 (1989).
- [28] P. Nason, S. Dawson and R.K. Ellis, Nucl.Phys., B **3335**, 260(E) (1989)
- [29] R.D. Field, R.P. Feynman, Phys.Rev.D **15** (1977) 2590.
- [30] R.P. Feynman, R.D. Field, and G.C. Fox, Nucl.Phys.B **128** (1977) 1.
- [31] R.P. Feynman, R.D. Field, and G.C. Fox, Phys.Rev.D **18** (1977) 3320.
- [32] M.L. Mangano, Physics-Uspekhi, **53** (2010) 109.
- [33] S. Albino, B.A. Kniehl, G. Kramer (AKK08), Nucl.Phys. B**803** (2008) 42.
- [34] B. Kniehl, G. Kramer, I. Schienbein and H. Spiesberger, Eur.Phys.J. C**72** (2012) 2082; arXiv:1202.0439v1 (2012) [hep-ph] .
- [35] ATLAS Collaboration; arXiv:1109.1403 [hep-ex].
- [36] T.P. Stavreva, and J.F. Owens, Phys.Rev. D **79** (2009) 054017; arXiv:0901.3791 [hep-ph].
- [37] A.V.Lipatov, M.A.Malyshev, N.P.Zotov, JHEP, **1205** (2012) 104; arXiv:1204.3828 [hep-ph].
- [38] T. Sjostrand,S. Mrenna and P.Z. Skands, Comput.Phys.Commun.,**178** (2008) 852.